J Mater Sci (2015) 50:2113–2121
DOI 10.1007/s10853-014-8773-3

Highly efficient adsorption of heavy metals from wastewaters by graphene oxide-ordered mesoporous silica materials

Xuemei Wang · Yifei Pei · Muxin Lu · Xiaoquan Lu · Xinzhen Du

Received: 18 October 2014 / Accepted: 4 December 2014 / Published online: 11 December 2014

Abstract Novel graphene oxide-ordered mesoporous silica materials with two-dimensional mesoporous structure and large surface area were successfully fabricated through sol–gel and self-assembly methods. The synthesized materials were characterized by small-angle X-ray diffraction, scanning electron microscopy, transmission electron microscopy, and nitrogen adsorption–desorption. By taking advantage of the excellent properties, the hybrid materials were employed as the adsorbent for removal of heavy metals in environmental waters by adsorption separation—inductively coupled plasma mass spectrometry. The results showed that the materials exhibited superior adsorption capacity, the removal efficiencies for As, Cd, Cr, Hg, and Pb reached 97.7, 96.9, 96.0, 98.5, and 78.7 %, respectively. The facile, low-cost, and environmental friendly synthesis method as well as highly efficient adsorption ability made it become a promising adsorbents for the removal of toxic heavy metals at low or trace concentrations from wastewater.

Introduction

Heavy metals have caused various diseases and threaten ecosystem and public health seriously with the rapid development of the industry in recent years [1]. They can be distinguished from other toxic pollutants, since their bioaccumulation and high toxicity even at very low concentrations in water [2, 3]. Therefore, the removal of heavy metals have attracted increasing attention and become an extensive research subject. Conventional treatment techniques, such as ion exchange, chemical precipitation, solvent extraction, and adsorption have been widely applied [4–6]. Among them, the adsorption is considered to be the most facile and effective method [7, 8].

Traditional adsorbents, such as clays [9], nanosized metal oxides [10], polymer and polymer-based hybrids [11, 12] were of interest for wastewater treatment. However, these classical adsorbents had several problems such as unpredictable metal ions removal, toxic sludge production, and extra handling cost for sludge disposal [13]. Moreover, most of sorbents were only applied to high or moderate concentrations of heavy metals but not to low or trace [14]. Therefore, it is very urgent to develop novel adsorbents with low-cost, simple operating performance, and excellent adsorption efficiency to low or trace.

In recent years, with progresses in modern nano-science and technology, ordered hybrid porous materials have exhibited substantial performance in adsorption and separation applications because of regular, uniform, and interpenetrating mesopores, tunable pore sizes, high surface areas [15–18]. Numerous organic–inorganic porous hybrids have been developed for removing heavy metal ions from wastewater, such as Cd, Cu, Hg, and Pb [19–22]. In addition, as an attractive 2D material with remarkable physical and chemical properties, graphene oxide (GO) composites have been widely applied in this field [23–25].

In this study, in order to take good use the advantages of GO and porous materials, graphene oxide-ordered mesoporous silica materials (denoted as GO-OMS) with long

Electronic supplementary material The online version of this article (doi:10.1007/s10853-014-8773-3) contains supplementary material, which is available to authorized users.

X. Wang (✉) · Y. Pei · M. Lu · X. Lu · X. Du
College of Chemistry and Chemical Engineering, Northwest Normal University, Lanzhou, China
e-mail: wxm98@163.com

X. Wang · X. Lu · X. Du
Key Laboratory of Bioelectrochemistry & Environmental Analysis of Gansu Province, Northwest Normal University, Lanzhou 730070, China

mesoporous channels and high surface area were prepared through sol–gel and self-assembly methods. The mesoporous material was dispersed into the surface of the graphene sheets, not only could the graphene and the porous material maintain the inherent characteristics of each, but also produced a novel synergistic effect. By taking advantage of these merits, the novel materials were utilized to remove heavy metals (As, Cd, Cr, Hg, and Pb) from complex real wastewater samples with high efficiency in spite of the low or trace concentration. The process of this work was depicted in Supplementary Figure S-1.

Materials and methods

Materials and chemicals

Sodium nitrate ($NaNO_3$), Nitrate (HNO_3, 98 %), Sulfuric acid (H_2SO_4, 98 %), Hydrochloric acid (HCl, 37 %) were bought from YanTai chemical Co. Ltd. (Shandong, China); Ethanol (C_2H_5OH, 99 %) and Potassium permanganate ($KMnO_4$) were purchased from Tianjin KaiTong chemical reagent Co. Ltd. (Tianjin, China); Graphite powder was obtained from Shanghai ShanPu chemical Co. Ltd. (Shanghai, China); Tetraethyl orthosilicate (TEOS, 99 %) was purchased from ZhongQin chemical reagent Co. Ltd. (Shanghai, China). Pluronic P123 was obtained from Sigma-Aldrich (Steinheim, Germany). All used deionized water in the experiment were prepared by Aquapro Water Purification System (Chongqing, China). All chemicals were of analytical grade and used without further purification.

The individual standard stock solutions of As, Cd, Cr, Pb, and Hg (1 mg/mL) were supplied by National Institute of Metrology (China) and stored at 4 °C. The working standard solution was prepared by combining aliquots of each individual stock solution and diluting by 2 % HNO_3 solution to obtain a desired concentration. Fresh working solutions were prepared daily by appropriate dilution of the stock solutions.

Two wastewater samples were collected from Dongda River (Industrial wastewater) and Xida River (Domestic sewage) (Baiyin, Gansu Province, China). All these samples were filtrated through 0.45 μm glass fiber membrane (Automatic Science, China) and stored in brown glass bottles at 4 °C.

Synthesis of graphene oxide (GO)

GO was synthesized according to modified Hummers method [26]. 1.0 g graphite powder, 1.0 g $NaNO_3$, and 46 mL H_2SO_4 (98 %) were stirred in an ice bath for 0.5 h. Next, 3.0 g of $KMnO_4$ was added slowly. Once these were mixed, the ice bath was removed and the suspension was stirred for 2 h at 35 °C. Next, 46 mL of water was added dropwise under vigorous stirring about 20 min. Then, 10 mL H_2O_2 (30 %) was added slowly. The mixture was centrifuged at 4000 rpm and washed with 5 % HCl (v/v). Subsequently, the sediment was washed with deionized water and centrifuged at 8000 rpm. The final sediment was dried at 60 °C in a vacuum drier for 24 h and redispersed in deionized water with ultrasonication for 2 h to make GO solution.

Preparation of graphene oxide-ordered mesoporous silica (GO-OMS)

The typical preparation approach for GO-OMS is shown in Scheme 1. Briefly, H_2SO_4 (1.7 mL, 98 wt%) and P123 (1.0 g, MW = 5800) were dissolved in 30 mL of distilled water by vigorous stirring under 40 °C to form a homogeneous solution. Then a certain amount of as-prepared GO (weight from 0, 20, 60 to100 mg) was added and homogeneously dispersed under sonication, followed by adding dropwise 2.3 mL TEOS and stirred under 40 °C for 20 h. The resulting black mixture was transferred into a Teflon-lined autoclave, heated at 100 °C for 24 h before it was cooled down to room temperature. The products were precipitated through centrifugation, further purified by distilled water and ethanol, then dried at 80 °C in a vacuum drier for 3 h. Finally, the powder was carried out in a tubular furnace at 550 °C for 5 h under a flow of nitrogen with a low rate to remove the templates P123 and form GO-OMS.

The final samples were labeled as GO-OMS-x (x = 20, 60, 100) and x represents different weight GO was added. For comparison, the prepared ordered mesoporous silica without GO was labeled as OMS.

Removal of heavy metals

The removal of heavy metals by GO-OMS-x was conducted by the batch equilibrium method in an E24 Incubator Shaker (New Brunswick Scientific). 0.10 g of GO-OMS was added to 50 mL real wastewater samples containing different concentrations (the initial concentrations) of heavy metals (Table 1). The mixtures were stirred at room temperature (25 ± 2 °C) for 24 h to ensure sorption equilibrium. After 24 h, the conical flasks were removed and solution filtered using a 0.45 μm glass fiber membrane. The filtered solution was analyzed for the final concentration (Table 1). The operating condition for ICP-MS is listed in Supplementary Table S-1 of the Supporting Information. For all of the ICP-MS determinations, the data are presented as averages of three measurements with relative standard deviations (RSDs) of less than 5 %. Heavy

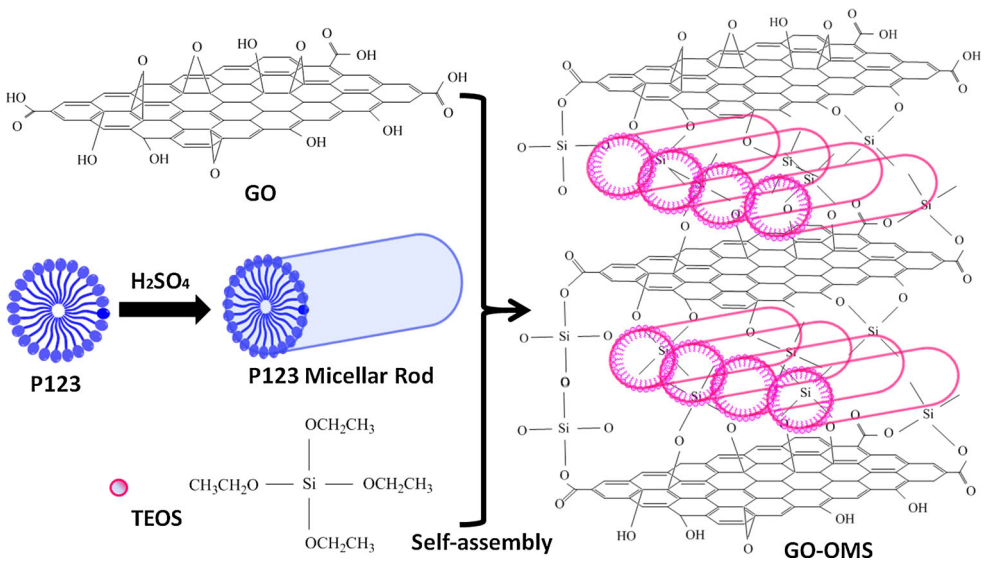

Scheme 1 Synthesis Route to Graphene Oxide-ordered mesoporous silica (GO-OMS)

Table 1 The concentration of heavy metals in the wastewater before and after different materials adsorption

Materials	Dongda river (industrial wastewater)					Xida river (domestic sewage)				
	As[a]	Cd	Cr	Hg	Pb	As	Cd	Cr	Hg	Pb
Original solution[b]	421.50	58.71	78.58	1.20	200.90	176.20	3.82	14.10	0.20	0.47
AC	127.80	25.31	52.98	0.21	152.60	17.51	0.27	10.47	0.08	0.25
OMS	37.10	10.21	26.94	0.03	121.00	6.62	0.25	6.35	0.01	0.16
GO-OMS-20	30.20	9.00	14.62	0.01	112.30	4.03	0.12	0.57	0.003	0.10
GO-OMS-60	52.20	16.67	16.67	0.05	133.30	4.53	0.19	3.52	0.06	0.17
GO-OMS-100	86.85	15.54	15.64	0.07	144.20	6.10	0.25	3.29	0.05	0.13

[a] The unit of concentration of five heavy metals is ppb (μg/L)

[b] The concentration of original solution is the initial concentration (μg/L)

metals removal efficiency was calculated using the following equation.

$$\text{Removal efficiency } (\%) = \frac{(C_0 - C_e)}{C_0} \times 100, \quad (1)$$

where C_0 and C_e are the initial and final concentrations of heavy metals in wastewater (μg/L), respectively. The removal efficiency of heavy metals were examined without pH adjustment. The ratio of mass and charge of each element (As, Cd, Cr, Hg, Pb) is listed in Supplementary Table S-2 of the Supporting Information.

Characterization

The OMS and GO-OMS-*x* ($x = 20$, 60, 100) were characterized with Small-angle X-ray diffraction (SAXRD), Scanning electron microscopy (SEM), Transmission electron microscopy (TEM), and Nitrogen adsorption–desorption. The SAXRD measurements were carried out on a D/max-2400 X-ray powder diffractometer (Japan, Rigaku), using Cu Kα radiation (40 kV, 30 mA) source with a resolution of 0.02° and scanning speed of 0.5°/min. SEM images were recorded on a ULTRA Plus (Germany Zeiss), operated under high vacuum conditions, to visualize the morphology and size distribution of the particles. TEM conducting on Tecnai G2 F20 (FEI,USA) with an accelerating voltage of 80 kV was used. Carbon coated copper grids were used for the TEM sample preparation. Samples were dispersed in ethanol and applied as droplets to the grids. Nitrogen adsorption–desorption isotherms were performed at 77 K on a Quantachrome AS1Win™. The sample was first degassed at 120 °C for 5 h before adsorption measurements. The specific surface area was calculated from the adsorption–desorption isotherm using the Brunauer–Emmet–Teller (BET) equation and the pore size was calculated from the adsorption isotherm by applying the Barrett–Joyner–Halenda (BJH) method. Heavy metals (As, Cd, Cr, Hg, Pb) concentrations were determined by inductively coupled plasma mass spectrometry (ICP-MS) on Thermo Element ICP-MS XSERIES 7.

Results and discussion

Characterization of OMS and GO-OMS

Nitrogen adsorption–desorption isotherms

To investigate the textural parameters of the OMS and GO-OMS-*x* materials, nitrogen adsorption–desorption isotherms were performed and the results are shown in Fig. 1 and Table 2. Figure 1 exhibited the prominent characteristic of type-IV isotherms with a distinct hysteresis loop of H1 in the P/P_0 range of 0.4–1.0, which implied the presence of relatively large mesopores in the frameworks. The mesopore size were calculated by the BJH method ranges from 5.02 to 6.32 nm with a narrow distribution for samples, which indicated the materials had very uniform mesoporous structure. Moreover, the capillary-condensation step for GO-OMS-*x* was significantly shifted to lower relative pressure with the increase of GO weight, showing a gradually decreases in the pore size, which was quite consistent with the XRD results. As shown in Table 2, the structure parameters of GO-OMS-*x* decreased slightly because of the introduction of GO in the OMS. However, the textural parameters of GO-OMS-*x* compared to that of OMS were improved obviously because of the ultra-high surface area of GO. For example, the surface area and the pore volume of GO-OMS-20 were twice as high as the OMS, which contribute to the incorporation of GO.

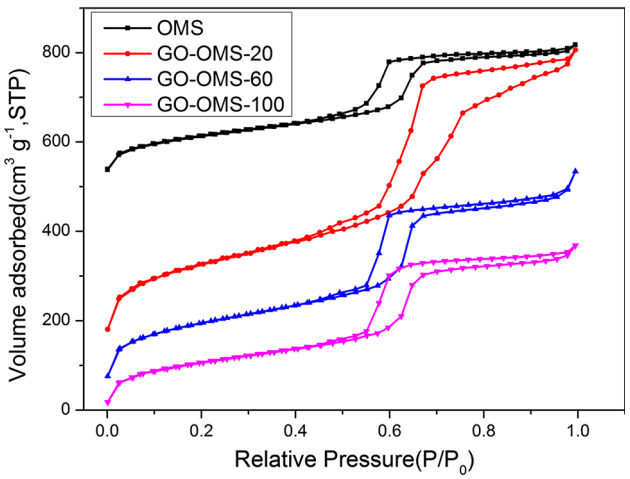

Fig. 1 N_2 adsorption–desorption isotherms of OMS and GO-OMS-*x* (*x* = 20 mg, 60 mg, 100 mg) samples

Table 2 The structure parameters of OMS and GO-OMS-x (*x* = 20, 60, 100 mg) samples

Samples	BET surface area (m^2/g)	Pore volume (cm^3/g)	Pore size (nm)
OMS	434.42	0.59	5.05
GO-OMS-20	872.90	1.28	6.32
GO-OMS-60	799.28	0.97	5.02
GO-OMS-100	589.55	0.74	4.76

SAXRD patterns

The mesoporous structure of samples were investigated by SAXRD and shown in Fig. 2. A well-resolved diffraction peak corresponding to (100) indicated the existence of highly ordered two-dimensional hexagonal mesostructure with the space group of p6 mm, except for GO-OMS-100. It is revealed that the presence of GO had an influence on the self-assembly of the tri-block copolymer. As a result, no obvious diffraction peak was observed for GO-OMS-100. What is more, the XRD reflections shifted in the direction of lower 2θ values along with the enhanced weight of GO, which reflected an expand in d-spacing and unit-cell size of the mesoporous materials [27].

SEM images

The SEM images of OMS and GO-OMS-*x* are shown in Fig. 3. It could be seen that almost all synthesized materials exhibited honeycomb-like morpha and porous structures (Fig. 3a–c), which were beneficial to heavy metals adsorption in that the pores increase the surface area of the materials leading to easy migration of metal ions into the interior of the composites. It might be due to the excess addition of GO could cause agglomeration of the graphene sheet and thus negatively affect the mesostructure for GO-OMS-100 (Fig. 3d). The dosage of GO was responsible for mesophase of the structure and had impact on the performance of the material. Consequently, in order to prevent the GO from aggregating and restacking, the optimum dosage of

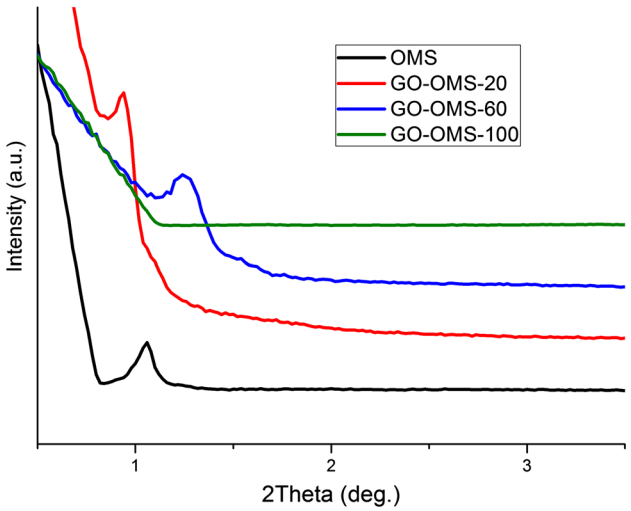

Fig. 2 Small-angle XRD patterns of OMS and GO-OMS-*x* (*x* = 20 mg, 60 mg, 100 mg) samples

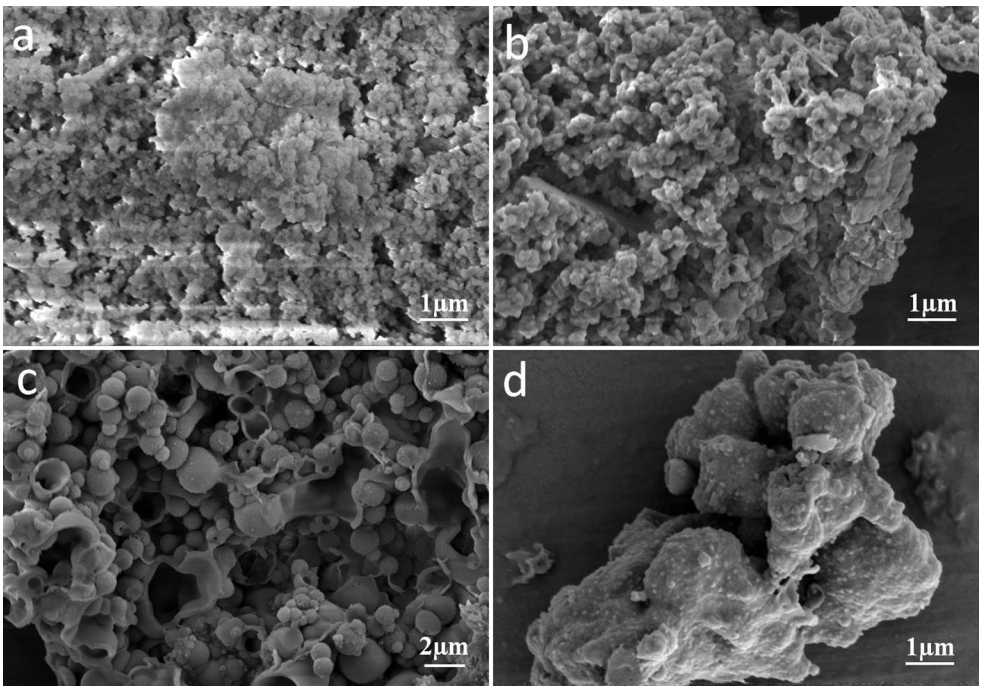

Fig. 3 SEM photographs of **a** OMS, **b** GO-OMS-20, **c** GO-OMS-60, and **d** GO-OMS-100 samples

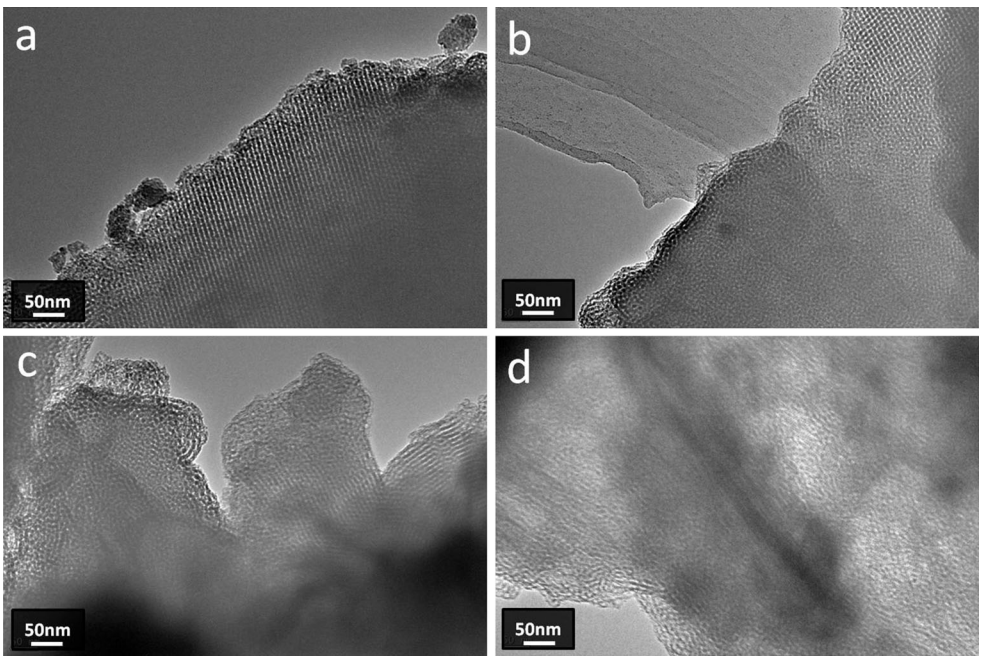

Fig. 4 TEM micrographs of **a** OMS, **b** GO-OMS-20, **c** GO-OMS-60, and **d** GO-OMS-100 samples

GO was 20 mg, the materials could keep both the mesostructure of OMS and high mechanical strength of GO.

TEM images

The morphology study was carried out with TEM. It is clearly seen in Fig. 4a–c that the OMS and GO-OMS-x ($x = 20$ mg, 60 mg) kept an ordered mesoporous channel, while GO-OMS-100 (Fig. 4d) had poor ordered mesoporous structure because of the over-adding GO, which were corresponding to the results from SAXRD and BET. Additionally, Fig. 4b–d illustrated that mesoporous silica were widely covered with thin transparent GO sheets, which demonstrated GO modified highly ordered

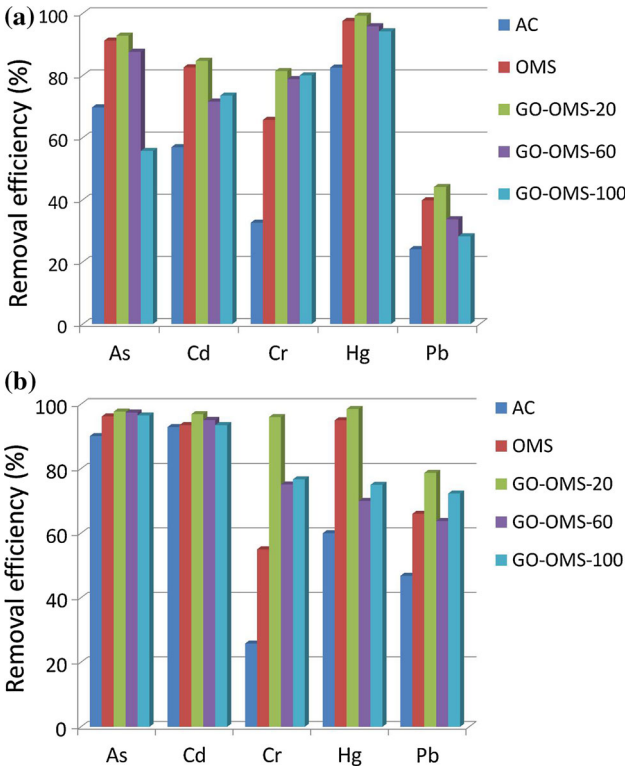

Fig. 5 The removal efficiency of five heavy metals to two real wastewater samples **a** Dongda River (Industrial wastewater), **b** Xida River (Domestic sewage)

mesoporous silica composites could be successfully prepared.

Analytical performance

Supplementary Table S-3 summarized the results of method validation. According to the definition of IUPAC, the detection limit ($S/N = 3$) of this method for As, Cd, Cr, Hg, and Pb were 0.05, 0.02, 0.10, 0.001, and 0.03 μg/L, respectively. The line arrange for As, Cd, Cr, Hg, and Pb were 0.20–500, 0.05–500, 0.35–500, 0.001–500, and 0.05–500 μg/L, respectively. The precision of the adsorption separation—ICP-MS method was assessed by five parallel adsorption of the analytes (0.5 μg/L). The results showed that the RSDs were <4.80 %, which demonstrated that good reproducibility could be achieved by the method.

Removal performance of heavy metals

In order to test and assess the applicability of GO-OMS composites, the removal efficiency of Lvyuan activated carbon (AC), the OMS and GO-OMS-*x* for five heavy metals (As, Cd, Cr, Hg, Pb) to two real wastewater samples are compared in Fig. 5. It should be mentioned that the two environmental water samples have not been studied at the adsorption and separation of heavy metals before. It could be seen that the AC had the lowest removal efficiency compared with the synthesized materials. All as-made materials showed superior removal capacities to five heavy metals, especially GO-OMS-20 displayed highest adsorption ability than the others, which due to the improvements of GO-OMS materials in physic-chemical characteristics as specific surface area, total volume of porous, more organic functional groups of GO. The concentrations of all heavy metals in domestic sewage sample after GO-OMS adsorption were lower than the GB/T5750-2006 (China, heavy metals ≤10 μg/mL). These results further verified that the GO-OMS had obviously positive effects on removal capacities to heavy metals of low or trace concentrations.

Real samples analysis

To estimate possible matrix influences, the two environmental samples after adsorbed by GO-OMS-20 were spiked with five heavy metals at two different concentration levels (0.5 and 10 μg/L) and analyzed by the proposed method. As listed in Table 3, the recoveries were in the

Table 3 Recoveries of real water samples spiked with the target analytes ($n = 3$)

Analyte	Concentration added (μg/L)	Dongda river (industrial wastewater)		Xida river	
		Recovery(%)	RSD(%)	Recovery(%) (100 %)	RSD(%)
As	0.5	77.1	6.2	93.9	4.9
	10	85.6	5.4	91.5	3.6
Cd	0.5	108.5	6.6	86.5	4.3
	10	111.2	7.7	103.4	5.5
Cr	0.5	108.5	9.1	91.2	4.8
	10	76.7	7.3	88.6	5.3
Hg	0.5	114.2	9.6	106.3	6.2
	10	109.5	8.5	108.7	5.4
Pb	0.5	88.5	6.4	87.4	5.6
	10	84.6	7.0	83.2	4.3

Table 4 Kinetic parameters for the Adsorption of five heavy metals onto GO-OMS-20 sample

Analyte	$q_{e,exp}$ (mg/g)	Pseudo-first-order kinetics (industrial wastewater)			Pseudo-second-order kinetics		
		k_1 (h^{-1}) (h^{-1})	$q_{e,cal}$ (mg/g)	R^2	k_2 g/(mg h^{-1})	$q_{e,cal}$ (mg/g)	R^2
As	47.3	2.049	74.10	0.9428	0.0071	44.10	0.9879
Cd	48.0	2.155	69.25	0.9382	0.0062	50.67	0.9678
Cr	45.5	1.7187	72.85	0.9359	0.0080	52.88	0.9901
Hg	49.0	1.103	84.20	0.9325	0.0108	48.21	0.9956
Pb	39.5	2.010	60.01	0.9489	0.0084	39.97	0.9903

range of 83.2–108.7 % for domestic sewage sample and 76.7–114.2 % for industrial wastewater water sample. These satisfactory recoveries indicated no significant effects from the matrix composition of the environmental water samples.

Durability of GO-OMS

In order to evaluate the durability and application of GO-OMS, the optimum GO-OMS-20 was collected after the heavy metals adsorption of two environmental samples and regenerated through washed by distilled water and ethanol, then dried at 80 °C in a vacuum drying oven for 3 h. The regeneration materials were characterized by SAXRD (Supplementary Fig. S-2), SEM (Supplementary Fig. S-3) and TEM (Fig. S-4). The results showed the regenerative materials still exhibited long range order mesoporous structure and the value of putting this material into use.

Adsorption kinetics

Batch kinetic studies were carried out using an accurately weighed 0.10 g portion of GO-OMS-20 in 50 mL of a solution of 100 mg/L five heavy metals, respectively. After the solution had been stirred for 24 h, the remaining heavy metal concentration was determined. The obtained experimental data were analyzed with pseudo-first-order and pseudo-second-order models as follows [28]:

The pseudo-first-order equation is given by

$$\frac{1}{q_t} = \frac{k_1}{q_e t} + \frac{1}{q_e}, \tag{2}$$

where k_1 (h^{-1}) is the pseudo-first-order adsorption rate constant, and q_e and q_t (mg/g) are the amounts of heavy metals adsorbed at equilibrium and time t (h), respectively.

The pseudo-second-order equation can be expressed as

$$\frac{t}{q_t} = \frac{1}{k_2 q_e^2} + \frac{t}{q_e}, \tag{3}$$

where k_2 [g/(mg h^{-1})] is the pseudo-second-order adsorption rate constant.

The kinetic parameters and models for adsorption of five heavy metals by GO-OMS-20 sample are summarized in Table 4 and Supplementary Figure S-5, respectively. Based on Table 4, it could be seen that the pseudo-second-order model provides better correlation coefficients than the pseudo-first-order model for the adsorption. Moreover, the good agreement between the calculated equilibrium adsorption capacities ($q_{e,cal}$) and the experimental values ($q_{e,exp}$) suggests that the pseudo-second order model is more suitable to describe the adsorption kinetics of five heavy metals. The pseudo-second-order model assumes that two reactions are occurring. The first is fast and reaches equilibrium quickly, and the second is slow and continues for a long time. The two reactions can occur either in sequence or in parallel. According to the conclusion by Saeid Azizian [29], the new adsorbents with pseudo-second-order adsorption kinetics may be applied in metal ion solutions of low initial concentrations.

Adsorption isotherms

Adsorption isotherms were determined to establish the model of adsorption and reveal the adsorption characteristics at a constant temperature. In this study, the Langmuir and Freundlich isotherm equations were used to evaluate the adsorption isotherms of the GO-OMS materials toward heavy metals.

The Langmuir isotherm equation assumes that the adsorption sites are distributed uniformly on the whole surface of the adsorbent and that only one adsorbate molecule is adsorbed onto each adsorption site [30]. Therefore, the Langmuir model is often used to evaluate monolayer adsorption at the interface between solid and liquid phases in dilute solutions. The linear Langmuir isotherm equation is expressed as

$$\frac{C_e}{q_e} = \frac{1}{k_L q_L} + \frac{C_e}{q_L}, \tag{4}$$

where q_e (mg/g) is the adsorption capacity, C_e (mg/L) is the equilibrium concentration of heavy metal in liquid phase, q_L (mg/g) and k_L (L/mg) represent the monolayer adsorption capacity and equilibrium constant for the adsorption, respectively.

The Freundlich model is applicable to both monolayer (chemisorption) and multilayer adsorption (physisorption), the Freundlich isotherm equation is an empirical equation and describes adsorption on heterogeneous surfaces [31]. The linear Freundlich isotherm equation is expressed as

$$\ln q_e = \ln k_F + \frac{\ln C_e}{n}, \quad (5)$$

where k_F (mg/g) is the binding energy constant reflecting affinity of adsorbents to heavy metal and n is the Freundlich exponent related to adsorption intensity.

In Supplementary Table S-5 shows the Langmuir and Freundlich isotherm parameters for the adsorption of five heavy metals onto GO-OMS-20 adsorbent at different temperatures. The coefficients (R^2) of the Langmuir (R_L^2) and Freundlich (R_F^2) indicated that the Langmuir isotherm fitted the experimental data better than the Freundlich model at a given temperature. This suggested that the mechanisms for the adsorbents were monolayer adsorption and chemisorption, the GO and mesoporous silica adsorbents can be effectively utilized in the adsorption processes.

Conclusions

In this work, GO-OMS was successfully fabricated. The as-made materials were clearly covered by thin oxide graphene sheets and exhibit ordered two-dimensional and honeycomb-like mesostructure with high surface area (872.9 m^2/g), uniform pore size (6.3 nm), and large pore volume (1.28 cm^3/g). On the basis of the excellent property of GO-OMS, the GO-OMS-20 exhibited superior removal capacity of heavy metals to domestic sewage such as As, Cd, Cr, Hg, and Pb, with equilibrium removal efficiencies of 97.7, 96.9, 96.0, 98.5, and 78.7 %, respectively. Therefore, the environmental friendly GO-OMS composites were expected to be used as low-cost and effective adsorbent for the removal of toxic heavy metals from wastewater even though at low or trace concentrations.

Acknowledgements This work was generously supported by the Natural Science Foundation of China (Nos. 21467028, 21107086, 21265019, 21265018, and 21327005), the Program for Chang jiang Scholars and Innovative Research Team, Ministry of Education, China (Grant No. IRT1283); the Program for Innovative Research Group of Gansu Province, China (Grant No. 1210RJIA001), Key Laboratory of Polymer Materials of Gansu Province and the Key Laboratory of Ecological Environment Related Polymer Materials of Ministry of Education.

References

1. Water Quality for Ecosystem and Human Health. (2008) 2nd edn. UNEP GEMS/Water Programme: Burlington
2. Gundogdua A, Ozdesa D, Durana C, Buluta VN, Soylakb M, Senturka HB (2009) Biosorption of Pb(II) ions from aqueous solution by pine bark (Pinusbrutia Ten.). Chem Eng J 153:62–67
3. Lourie E, Patil V, Gjengedal E (2010) Efficient purification of heavymetal- contaminated water by microalgae-activated pine bark. Water Air Soil Pollut 210:493–500
4. Fu FL, Wang Q (2011) Removal of heavy metal ions from wastewaters: a review. J Environ Manag 92:407–418
5. Tofighy MA, Mohammadi T (2011) Adsorption of divalent heavy metal ions from water using carbon nanotube sheets. J Hazard Mater 185:140–147
6. Qu RJ, Sun CM, Ma F, Zhang Y, Ji CN, Xu Q, Wang CH, Chen H (2009) Removal and recovery of Hg(II) from aqueous solution using chitosan-coated cotton fibers. J Hazard Mater 167:717–727
7. Qu RJ, Zhang Y, Qu WW, Sun CM, Chen J, Yin P, Chen H, Niu YZ (2013) Mercury adsorption by sulfur- and amidoxime containing bifunctional silica gel based hybrid materials. Chem Eng J 219:51–61
8. Chen J, Qu RJ, Zhang Y, Sun CM, Wang CH, Ji CN, Yin P, Chen H, Niu YZ (2012) Preparation of silica gel supported amidoxime adsorbents for selective adsorption of Hg(II) from aqueous solution. Chem Eng J 209:235–244
9. Gatica JM, Vidal H (2010) Non-cordierite clay-based structured materials for environmental applications. J Hazard Mater 181:9–18
10. Hua M, Zhang SJ, Pan BC, Zhang WM, Lv L, Zhang QX (2012) Heavy metal removal from water/wastewater by nanosized metaloxides: a Review. J Hazard Mater 211:317–331
11. Pan BJ, Pan BC, Zhang WM, Lv L, Zhang QX, Zheng SR (2009) Development of polymeric and polymer-based hybrid adsorbents for pollutants removal from water. Chem Eng J 151:19–29
12. Xia Y, Li YC (2002) Study of gelatinous supports for immobilizing inactivated cells of *Rhizopus oligosporus* to prepare biosorbent for lead ions. Int J Environ Stud 5:1–15
13. Babel S, Kurniawan TA (2003) Low-cost adsorbents for heavy metals uptake from contaminated water: a review. J Hazard Mater 97:219–243
14. Cossich ES, Tavares CRG, Ravagnani TMK (2002) Biosorption of chromium (III) by *Sargassum* sp biomass. Electron J Biotechnol 5:133–158
15. Wang XM, Liu JY, Liu AF, Liu Q, Du XZ, Jiang GB (2012) Preparation and evaluation of mesoporous cellular foams coating of solid-phase microextraction fibers by determination of tetrabromobisphenol A, tetrabromobisphenol S and related compounds. Anal Chim Acta 753:1–7
16. Coasne B, Galarneau A, Pellenq RJM, Di Renzo F (2013) Adsorption, intrusion and freezing in porous silica: the view from the nanoscale. Chem Soc Rev 42:4141–4171
17. Sherif AES (2009) Organic-inorganic hybrid mesoporous monoliths for selective discrimination and sensitive removal of toxic mercury ions. J Mater Sci 44:6764–6774. doi:10.1007/s10853-009-3577-6
18. Sun NR, Deng CH, Li Y, Zhang XM (2014) Highly selective enrichment of N-linked glycan by carbon-functionalized ordered graphene/mesoporous silica composites. Anal Chem 86:2246–2250
19. Zhou YM, Jin Q, Hu XY, Zhang QY, Ma TS (2012) Heavy metal ions and organic dyes removal from water by cellulose modified with maleic anhydride. J Mater Sci 47:5019–5029. doi:10.1007/s10853-012-6378-2
20. Ma, Mercedes SH, Carmen SH, Enrique ER, Higinio JR (2014) The use of mesoporous silica in the removal of Cu(I) from the

cyanidation process. J Mater Sci. doi:10.1007/s10853-014-8603-7
21. Ma TY, Zhang XJ, Shao GS, Cao JL, Yuan ZY (2008) Ordered macroporous titanium phosphonate materials: synthesis, photocatalytic activity, and heavy metal ion adsorption. J Phys Chem C 112(8):3090–3096
22. Zhang XJ, Ma TY, Yuan ZY (2008) Titania-phosphonate hybrid porous materials: preparation, photocatalytic activity and heavy metal ion adsorption. J Mater Chem 17:2003–2010
23. Chandra V, Park J, Chun Y, Lee JW, Hwang IC, Kim KS (2010) Water-dispersible magnetite-reduced graphene oxide composites for Arsenic removal. ACS Nano 4(7):3979–3986
24. Lei YL, Chen F, Luo YJ, Zhang L (2014) Three-dimensional magnetic graphene oxide foam/Fe_3O_4 nanocomposite as an efficient absorbent for Cr(VI) removal. J Mater Sci 49:4236–4245. doi:10.1007/s10853-014-8118-2
25. Chandra V, Kim KS (2011) Highly selective adsorption of Hg^{2+} by a polypyrrole-reduced graphene oxide composite. Chem Commun 47:3942–3944
26. Yoo EJ, Okata T, Akita T, Kohyama M, Nakamura J, Honma I (2009) Enhanced electrocatalytic activity of Pt subnanoclusters on graphene nanosheet surface. Nano Lett 9:2255–2259
27. Vinu A (2008) Two-dimensional hexagonally-ordered mesoporous carbon nitrides with tunable pore diameter, surface area and nitrogen content. Adv Funct Mater 18:816–827
28. Zhou LM, Liu ZR, Liu JH, Huang QW (2010) Adsorption of Hg(II) from aqueous solution by ethylenediamine-modified magnetic crosslinking chitosan microspheres. Desalination 258:41–47
29. Azizian S (2004) Kinetic models of sorption: a theoretical analysis. J Colloid Interface Sci 276:47–52
30. Liu Y (2006) Some consideration on the Langmuir isotherm equation. Colloids Surf A 274:34–36
31. Taleb MFA, Mahmoud GA, Elsigeny SM, Hegazy EA (2008) Adsorption and desorption of phosphate and nitrate ions using quaternary (polypropylene-g-N, N-Dimethylamino ethylmethacrylate) graft copolymer. J Hazard Mater 159:372–379